JOURNAL OF SPACECRAFT AND ROCKETS
Vol. 40, No. 4, July–August 2003

Scalable Solar-Sail Subsystem Design Concept

David M. Murphy* and Thomas W. Murphey†
ABLE Engineering Company, Inc., Goleta, California 93117
and
Paul A. Gierow‡
SRS Technologies, Inc., Huntsville, Alabama 35806

A scalable solar-sail concept, which integrates recently developed gossamer coilable longeron mast technology, has been developed, providing simple reliable deployment and structural robustness with minimum weight. This sail system is also unique in that it is composed of tensioned membranes without the incorporation of catenaries. This simplification is made possible through a mathematical demonstration of the insignificance of structural wrinkles on propulsive effectiveness. The sail package is a mass-optimized propulsion subsystem that can be mounted to a general heritage spacecraft to provide continuous low-level thrust. The design baseline is a three-axis-stabilized four-quadrant 40-m-square sail with attitude controlled by gimbaling the spacecraft on an extended boom. Considerations for the baseline design definition and the resulting performance vs size are reviewed.

Nomenclature

A	=	square sail system size, m
AM0	=	air mass zero
a	=	wrinkle amplitude
C	=	effective column length, m
D	=	mast diameter, m
E	=	Young's modulus, N/m^2
I	=	cross-sectional moment of inertia, m^4
K	=	temperature, K
k	=	buckling load correction term
L	=	sail mast length, m
L_1	=	Earth–sun Lagrangian point
l	=	wrinkle wavelength
P_{cr}	=	critical buckling load of sail mast system
P_R	=	pressure on sail along sun line
P_s	=	critical buckling load for simply supported column
P_{wR}	=	pressure on wrinkled sail along sun line
S	=	solar insolation average, 1363 W/m^2 at AM0
T	=	temperature, C
T_h	=	tension in halyard, N
α	=	solar absorptivity of sail metalization
β	=	angle of halyard line to sail mast, radians
ε_b	=	thermal emissivity of sail back side
ε_f	=	thermal emissivity of sail front side
σ	=	Stefan–Boltzmann constant, 5.67×10^8 W/m^{2}K^4

Introduction

SOLAR-SAIL technology[1] has been identified as enabling for many exciting space missions. Solar propulsion can also provide significant cost savings for missions with high delta-V requirements such as the Heliopause Explorer and Solar Polar Imager. Non-Keplerian orbits can provide unique perspectives in missions such as the Geostorm Warning Mission. The Geostorm mission plan is to utilize a solar sail to allow a satellite to remain stable at a point closer to the sun than the L_1 point. Moderate sail performance would offer a valuable increase in the solar-storm warning time provided by the aging satellite currently in service.

The solar-sail requirements for the Geostorm mission might be the least challenging among near-term applications. The required sail performance is shown herein to be achievable with reasonable margins and a high degree of reliability. Furthermore, the present concept is shown to be readily scalable for application to a series of progressively more challenging missions planned by NASA, the National Oceanic and Atmospheric Administration, and the U.S. Department of Defense after the GeoStorm mission.

System technologies required for solar sailing have yet to be demonstrated successfully in space. Attempts have been made to deploy both spinning and three-axis-stabilized membrane reflectors. The Achilles heel of many membrane system development efforts to date has been the complexity and lack of heritage of the deployment technology. The present sail system utilizes a deployer with 100% flight success over more than 50 missions in the past three decades. A method has been identified to optimize this heritage deployable structure, referred to as a coilable, for the family of lightly loaded applications known as gossamer systems. The incorporation of graphite composite materials into the coilable allows the performance goals of sailcraft to be met with a robust deployment system.

However, the deployment and structural performance of a sail system are only two of the challenges to be met in configuring a successful sail subsystem. Unique technologies involving optical performance, environmental stability, thermal expansion and wrinkle management of the sail film, system dynamics and control strategies, and many other issues must be addressed for realistic minimum mass solutions. For example, much theoretical work has been accomplished in the area of sailcraft orbit dynamics modeling, but that work has generally assumed rigid-body motion because of lack of definition for the sail subsystem design. The present sail design is shown to lead to more predictable structural modes for sail sizes from 20 to 300 m (400 to 90,000 m^2).

Often attitude control is implemented with tip vanes canting. The present design provides attitude control through center-of-mass offset (vs the center-of-pressure location) achieved by gimbaling of the spacecraft off a short (sail-centered) boom. In the present paper a family of three-axis-stabilized sail configurations is reviewed and contrasted for implementation ease and performance. A four-quadrant square sail design is selected. The concept discussed herein is referred to as the scalable square solar-sail (S^4) system.

Received 20 September 2002; revision received 18 April 2003; accepted for publication 20 April 2003.

*Chief Research Engineer. Member AIAA.
†Research Engineer. Member AIAA.
‡Aerospace Technology Director. Member AIAA.

S[4] Design Description

System Configuration

General configurations for the sail shape and suspension,[2] such as in Fig. 1, were evaluated for their simplicity and performance potential. When studies were done in the late 1970s, a four-point configuration (where nonplanarity of the four masts allows a planar sail) was favored. This configuration allows a single sail, which is doubly folded when stowed. The deployment can be well controlled by opening the sail in one dimension at a time. However, sail tension loads the masts in bending, which requires more structure (mass) to avoid buckling than a column in pure compression. The same is true for the five-point option.

A striped architecture, suggested by Greschik and Mikulas[2] as a useful assumption to simplify sail stress distribution analysis (catenaries are not needed), was judged to require overly complex sail construction. And the multitude of attachments to the mast would be a detriment to mass minimization. This is true for both the striped architecture and the continuous connection approach. One of the primary desires for the present program was to construct a system with the highest potential for complete ground verification. Achieving this objective is greatly aided by separating the actions of the mast and sail deployment.

The proceeding arguments and other lesser concerns led to the selection of the quadrant option. New analytical techniques[3] demonstrated that structural wrinkling, which is prevalent without the use of catenaries, would have a negligible effect on propulsive efficiency. So, the baseline design is a sequentially deployed (masts in parallel, then sails in parallel) quadrant sail without catenaries, as shown in Fig. 2.

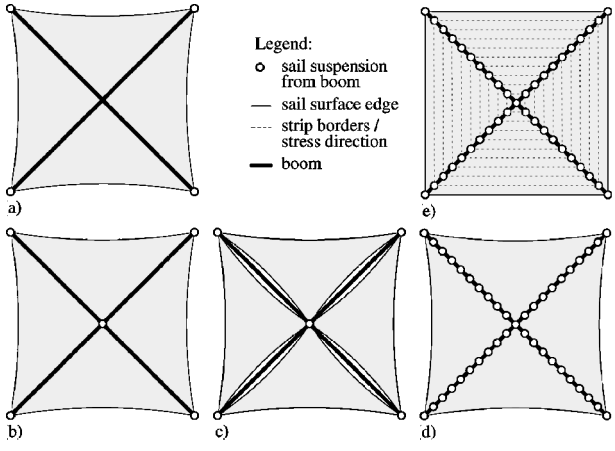

Fig. 1 General square sail configurations: a) four-point suspension, b) five-point suspension, c) separate quadrants, d) continuous connection, and e) striped architecture.

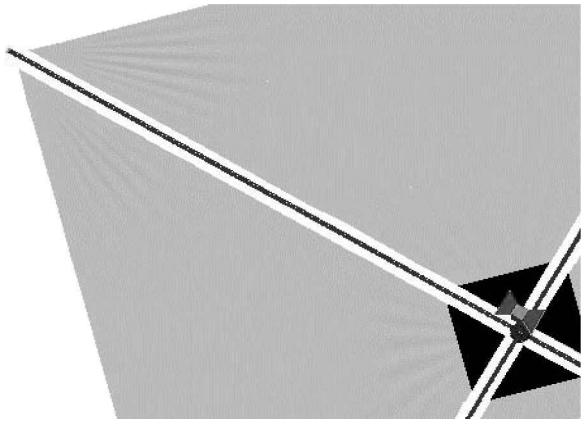

Fig. 2 Quadrant layout of S[4].

Sail Design

The sail quadrant design, developed by SRS Technologies, is a 5-μm-thick film construction with an aluminized reflective front surface and a black emissive back surface. The sail material is a unique polyimide, invented by NASA and commercialized by SRS, with extensive qualification test data and flight heritage. It has favorable structural characteristics and large-scale manufacturability.

The bulk form is soluble and can therefore be cast, yielding uniform thickness sheets with isotropic properties. SRS has developed carbon-based additives that can enhance the emissivity. Carbon loading is expected to be of additional benefit by increasing modulus and lowering the sail coefficient of thermal expansion (CTE). However, carbon loading presents numerous difficulties that are still under study. If the material cannot be developed and proven in time to support the first flight opportunity, the fallback will be to use the flight-proven basic material. The emissivity is greatly reduced, but is still sufficient for missions without close solar approach.

Another potential additive, under development by SRS, is a dewrinkling agent. Experiments have shown that by slightly enhancing the creep potential of the base material the packaging (material) wrinkles can be eliminated at low operating stresses.

A fold pattern that allows the quadrant to be packaged efficiently alongside the stowed masts was developed. The sail manufacturing methods and fold processes were experimentally explored with a subscale demonstrator. Deployment tests, as shown in Fig. 3, were repeatedly successful, yet the constraint provided by the floor is obviously nonconservative.

One goal of the present program was to configure a deployment scenario that is much more deterministic: All folds must be in a known, or narrowly constrained, position during deployment to avoid entanglement. No significant portion of the sail can be without tension, or solar pressure will quickly deform the sail shape. An example of a sequence with high deterministic qualities is discussed in a later section.

Rapid depressurization during the launch ascent can cause premature unfolding or structural overloading. Generally speaking, a two-dimensional fold pattern of a planar sheet leaves a short path for the escape of gases during depressurization. This was demonstrated in tests with a folded sail sample.

Prior to and during deployment the space thermal environment poses challenges to the sail. For example, between closed folds thermal extremes can cause entrapped water to freeze. Prior to launch, the entire subsystem must be bagged and supplied a continuous nitrogen overpressure to prevent moist air from infiltrating the packaged sail. A solar oven condition, formed by partially opened folds exposed to the sun, can be prevented with appropriate shading of the packaged portion of the sail.

The temperature (°C) of the deployed sail film (normal to the sun) can be derived from a simple heat-balance equation:

$$T = \left\{ \frac{\alpha S}{\left[AU^2 \sigma (\varepsilon_f + \varepsilon_b) \right]} \right\}^{\frac{1}{4}} - 273 \qquad (1)$$

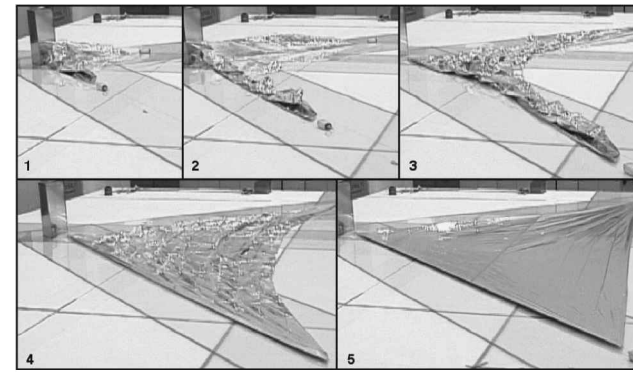

Fig. 3 Deployment of subscale quadrant.

If the sail is oriented off-sun, the temperature will drop only slightly, by the fourth root of the cosine. The absorptivity of the sail is minimized as a consequence of optimizing the aluminum reflectivity. The additional front-side coatings considered were not mass effective. The thin aluminum layer will allow a small portion to be transmitted: less than 1%. As the other factors in the analysis are all relatively fixed, the resulting temperature is primarily dependent on the emissivity of the film backside. Results for various emissivities as a function of solar distance in astronomical units (AU) are shown in Fig. 4.

Tests of sail samples with various carbon loading fractions demonstrated that a high emissivity—and thus a close solar approach capability—can be achieved. As can be seen in Fig. 2, the corner of the sails near the spacecraft would be left unmetallized. The high absorptivity of the carbon-loaded film will prevent two-times solar loading of the spacecraft.

Mast Design

The sail masts are an advanced version of a structure, which has flown repeatedly in space with 100% success. These robust and reliable structures, which can be coiled and stowed in less than 2% of their deployed length, are referred to as coilables. The coilable deployment is driven by internal stowed strain energy and limited by a lanyard in tension. In the present application rate limiting of all four masts is accomplished with a single motor. The tip end is biased to erect first, and the transition zone progresses away from the base as the lanyard is payed out (Fig. 5).

The coilable structure can be very mass efficient. Masts similar in diameter to the current application and which flew on the IMAGE spacecraft in 2000 weighed less than 100 g/m. Recent studies

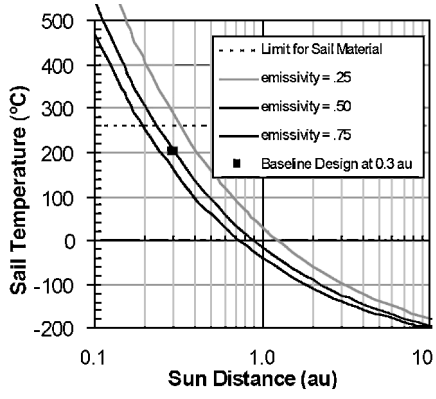

Fig. 4 Sail temperature vs AU: sail material allows closer solar approach than 0.3 AU.

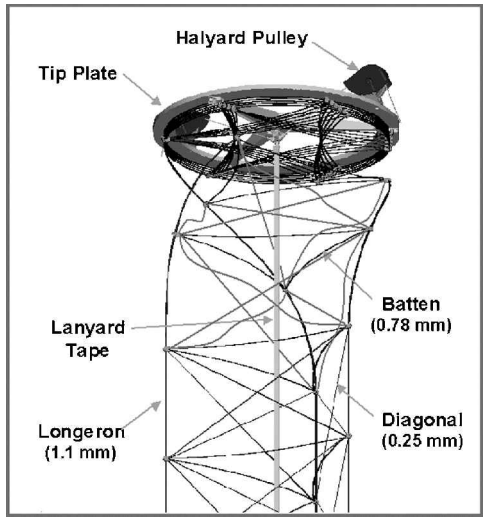

Fig. 5 Coilable mast description.

have shown that the mass efficiency of the coilable can be radically improved through the selection and proper proportioning of materials as appropriate for the needs of solar-sail applications. To form an "advanced" coilable, the heritage material for the longerons and battens, S2 fiberglass, are replaced by a modern carbon fiber composite. This is possible because the optimal boom proportions do not exceed the material strain limitations. The modulus is increased by 3.5 times with 20% lower density material. The packaging volume is reduced to less than 1% (of the deployed length). Further mass reductions are possible when the complexity and volume of the mast corner fittings are reduced. The part count per corner has been reduced from more than a dozen to a single molded fitting.

For the unique load regime of solar sails, the coilable is lighter than a min-wall gauge tube and very nearly as light as an isogrid tube.[4] Once the mass of deployment necessities; for example, inflation gas, valves and tanks, tube bladders and multilayer insulation, heaters, etc., is overlaid on an isogrid, the coilable is a clear mass winner.

The longerons are the primary structure of the mast and determine its key performance characteristics. The diagonals are tensioned by the buckled battens and serve to position the longerons relative to each other radially and axially. The materials and section properties of these separate elements can be optimized for any particular application. First, bending stiffness is a function of the longeron section properties, elastic modulus, and distance from the mast center. Second, bending strength is a function of the section properties and elastic modulus of a longeron, as well as the mast bay length. Third, shear and torsional stiffness are a function of the diagonal section properties, elastic modulus, and angle within the bay. Fourth, shear and torsional strength are developed by the buckling strength of the batten.

For the sailing application the shear and torsional stiffness and strength are of secondary importance. Consequently, batten and diagonal mass can be minimized as their primary role is now to provide sufficient support to the longeron to enforce the local buckling mode to within a single bay. The analysis for local buckling is then that of a simply supported Euler column, modified by any manufacturing tolerances that introduce straightness imperfections. The overall structure is mass optimized when the global buckling limit is equal to the local buckling limit. The global buckling calculation requires a more involved analysis than the local buckling as detailed in a later section on loadings and capability.

System Packaging

The packaged sails and masts are contained in a lightweight construction of graphite facesheets with aluminum honeycomb. The four masts are arranged symmetrically around a central bay that houses the stowed offset boom and two-axis gimbal. The remaining volume in the same plane is used to store the four sails. The arrangement is depicted in Fig. 6, where the structure and packed sails are sectioned to remove the top half to allow better viewing. Inserts on the top deck of the structure allow mounting of launch tiedown and release actuators.

In flight the sail masts would be both deployed and dynamically verified prior to the sails being raised on the halyard lines. Sequential

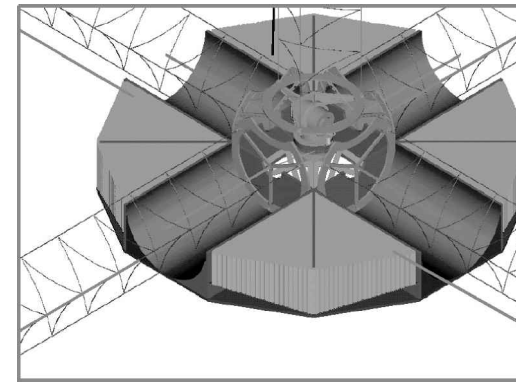

Fig. 6 Sectional view of central stowage structure.

operation simplifies mechanization, increases opportunities for better ground testing fidelity, and improves flight validation activities and reliability.

To minimize mass and increase reliability, the elements needed to secure the masts for launch, to synchronize their deployment, and to spring-tension the sails are shared. Furthermore, one motor is used to deploy the masts and sails and later to control offset boom rotation for attitude control. Because the four masts are identical and symmetrically arranged, the following discussion of the features of one applies to all.

The stowed mast occupies a cylindrical volume of 23 cm in diameter by 26 cm long (0.9% of the deployed mast volume). The mast longerons are coiled upon one another forming a stack well supported for launch that is preloaded by tensioning of the lanyard. The lanyard is fixed to the tip plate and runs through the center of the mast to a reel that is mounted around the rotary axis gimbal at the center of the stowage structure. The lanyards from each of the masts share this reel. The reel is grounded to the structure by dual shear pins that prevent the tiedown loads from being reacted through the gimbal gearbox.

The last meter of the lanyard (near the tip plate) is constructed of a high-load-capacity steel tape of sufficient length to allow several wraps to be wound onto the reel. The remainder of the 30-m-long lanyard is also steel, but of a reduced cross section that provides high margin over boom and sail deployment loads with a mass of only 3 g/m. The lanyard is constructed of two tapes laser welded together in a nearly continuous pattern for redundancy against imperfections or handling damage to this gossamer line.

System Deployment

After release from the launch vehicle, deployment operations would begin with unfolding of the solar arrays, followed by the extension of the spacecraft offset boom (Fig. 7). An animation of the ST7 deployment produced by M. Hart of the Aerospace Corporation can be seen at http://solarsail.jpl.nasa.gov/tasks/index.html. Deployment of the masts is initiated by the release of pin pullers on the lanyard reel. The first motion of the reel allows the preload in the mast stacks to be released. The motor is commanded to begin paying out the lanyards. Springs at the inboard end of the longerons bias the mast to uncoil from the base, and the transition section progresses out the mast until the tip completely unwinds. The stowed strain energy of the coiled longerons powers the deployment. The gimbal assembly constrains the rate and measures the travel.

The spacecraft attitude control system will be disabled during deployment of the masts and sails to eliminate undesired loading while the structure transitions many frequency regimes during deployment. The action of uncoiling the masts—at a rate of 2.5 cm/s—will occur over a 20-min period. Once the masts have fully deployed, they are ready to support the raising of the sails. But first, the spacecraft inertial system would be taken off standby, and a series of small inputs of attitude adjustment would be used to achieve three-axis stabilization and then to excite the masts and investigate/validate the

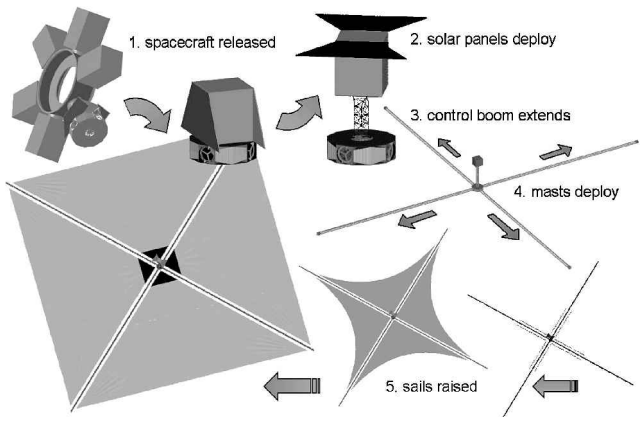

Fig. 7 Deploy sequence.

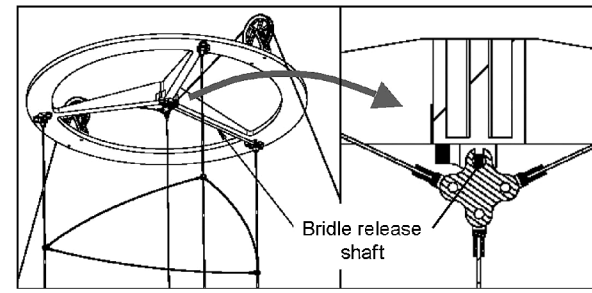

Fig. 8 Mast-tip detail: lanyard to halyard.

structure modes. Modal information would be developed from both spacecraft gyro data and imaging returned by panospheric cameras. This will also allow better correlation of modeling of the system modes observed during and after sail deployment.

At the end of mast deployment, the snap action of a longeron tip completing the last few degrees of rotation (to a position normal to the tip plate) will have released the bridle block (Fig. 8) that joins the lanyard to the two halyards that run back down the mast to the quadrant corners of the still stowed sails.

In the launch configuration the halyards are wrapped around the longeron so that during mast deployment they unwind and form a slack line from the mast tip to the stowed sail quadrants. When the mast assessment is complete, the second stage of system deployment, raising the sails, is initiated. The motor is commanded to turn in reverse and the lanyards are reeled in, which pulls the sails up as the halyards run over the tip pulleys and down the mast. All quadrants would follow this process simultaneously as they share the halyard drive mechanism housed in the central stowage structure.

Baseline Sail Deployment Method

Raising the sails will progress at a slow controlled pace, averaging less than 1 cm/s, over 60 min. The motor revolution count will indicate when the sails are nearly taught. The camera will be used to document the dynamics of the quadrants unfolding and verify the sails are nearly taught. Prior to sail deployment the spin rate of the momentum wheels should be near a maximum to inertially stabilize the spacecraft, with the control mast pointing at the sun, so that if the deploying sails billow under solar pressure they will move in a direction that poses the least risk of entanglement.

Tension is applied to all sails by a set of negator-style springs located in the central bay. Springs are needed to maintain the desired film stress as the sails cool and contract (33 cm relative to mast) during Earth eclipse (expansion is 25 cm at 0.3 AU). The negators are fully extended at launch and rotate with the reel (on the gimbal output) during mast and sail deployment. The reel, once decoupled from the negator carrier ring, will rotate around the gimbal body as the negators pull the remaining slack out of the sails. Decoupling is accomplished by actuating a small pin puller.

The negator springs will be designed to have a very low spring rate. The sail tension will vary only slightly over the travel induced by differential thermal growth between the sail and the mast. The overall spring travel allowance provided will be four times the expected thermal compliance to allow the motor position to be varied to change the sail tension. [The rotation of the motor needed for attitude control (+180 deg) is a small fraction of total negator motion.] The effect of sail flatness and frequency can then be explored.

The placement of the negators within the central mechanism allows a (redundant) set of springs to tension all sails equally. More importantly, this configuration and sequence leave the low compliance of the negators out of the halyard lines during the critical sail blanket deployment phase. The first solar-array blanket deployment on the International Space Station failed (extra vehicular activity intervention was required) because the sticking of folds was not anticipated. The compliance of the negator reels designed to tension the blanket from the base at full deploy, allowed strain energy to develop as the blanket was unfolding. When sections stuck, the springs extended fully as the mast continued to deploy. When the

springs reached end of travel stops, the mast motion pulled open the stuck fold. The negators then retracted, pulling the blanket back to collide with the base structure. This probably caused solar-cell fractures and eventually led to the negators jamming as a result of loss of containment.

Similarly for the solar-sail application, negator compliance would allow the force needed to open a sticky sail fold to be stored as a large amount of energy in an extended negator. The energy would be returned when the negator retracts, thus accelerating the blanket. It is clearly desirable to avoid such dynamics and potential failure modes. Therefore, the proposed mechanism introduces the negator, for final tensioning, after sail unfolding is complete.

Alternate Sail Deployment Method

The intrinsic flimsiness of the sail, coupled with the applied solar pressure loading, means that unconstrained portions of the sail are inherently risky during deployment. The potential motions cannot be reliably modeled. Twisting and wrapping of the sail around itself or the masts would surely lead to failure. Although the baseline method of deployment just described is well controlled, a sequence with a higher deterministic quality can be imagined, as shown in Fig. 9. All quadrants would follow this process in parallel as they share a halyard drive mechanism housed in the stowage structure. It might be worth the additional mechanism to incorporate this approach as the baseline.

Mast Loadings and Capability

The critical failure modes that affect mast sizing and mass are global and local buckling. To produce a robust design, a minimum factor of safety of three was chosen. The dimensions chosen for this point design dictate that the mast is global buckling limited. The global buckling load capability of a single mast of length L, which can be considered as a pin–pin column or equivalently as a cantilever beam in compression where the load is directed always towards the root, is

$$P_s = \pi^2 EI/L^2 \tag{2}$$

This simple so-called "follower load" case is not directly applicable to a square quadrant sail as the geometry of sail tensioning can cause the load to be directed at a point as far as $0.7L$ behind the root of a mast, as indicated in Fig. 10.

It is important to recognize the halyard angle β varies in flight as the sail changes size because of temperature. Although the negators function to maintain approximately the same tension, the variation in halyard angle changes the characteristic length C and hence the buckling load margin and quadrant frequency as well. As shown in Fig. 11, the highest frequency corresponds to a slightly higher halyard angle than the bisector angle.

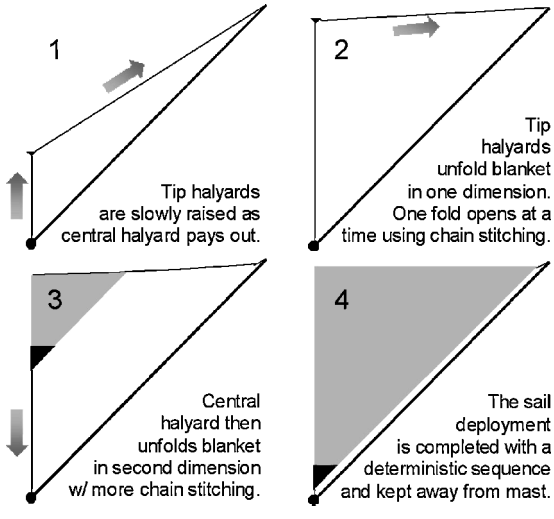

Fig. 9 Alternate sail deploy sequence.

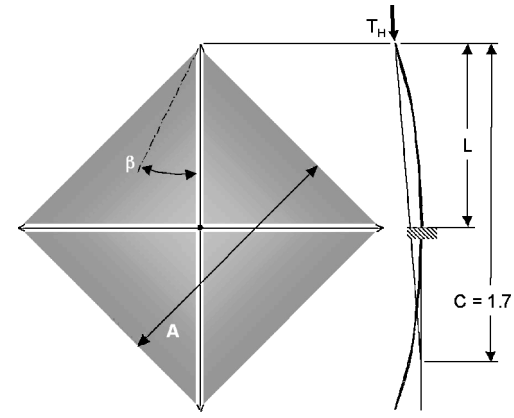

Fig. 10 Sail tension vector in mast plane.

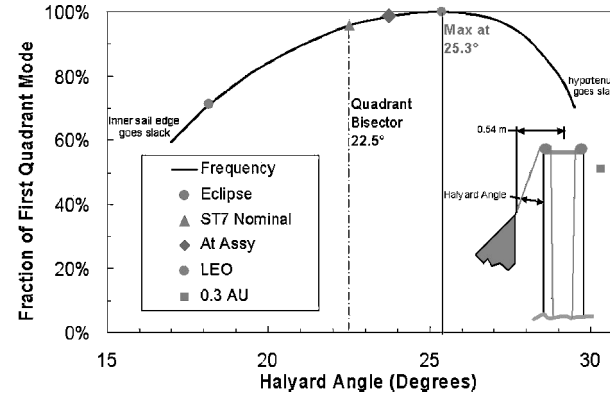

Fig. 11 Quadrant frequency vs load angle.

For the studied elliptical Earth-orbiting application it was chosen to maximize the frequency when the spacecraft was at perigee. This can increase controllability when orientation change is likely highest and the sail is facing larger disturbances such as magnetic field interaction. At perigee the sail is hottest. Other locations in the orbit correspond to lower halyard angles and thus lower frequency, as shown in Fig. 11.

For the simple case where the halyard angle bisects the sail corner and considering that all masts buckle at the same load, an inspection of the quadrant sail geometry reveals that

$$C/L = 1/[1 - \tan(\beta)] \tag{3}$$

With this knowledge of the location where the load is directed, the correct buckling load can be calculated. Timeshenko and Gere[5] provides the following transcendental relation to find the buckling load:

$$\tan(kL) = kL(1 - C/L) \tag{4}$$

where

$$k = (P_{\rm cr}/EI)^{\frac{1}{2}} \tag{5}$$

The results of this buckling calculation are shown in Fig. 12, where one can see that the change in buckling load is significant over the range of halyard angles that thermal extremes induce.

For a mission that includes close solar approach, the variation in buckling margin and sail frequency can be reduced by designing the sail with a larger gap between the masts and sails as this will reduce variations in halyard angle caused by sail thermal growth. However, this increases mast length.

Given the symmetrical arrangement of the masts in the plane of the deployed sails, it is tempting to analyze the statics of mast strength as a column under compression caused by sail tension alone (with the proper load direction correction as just discussed) as this is by

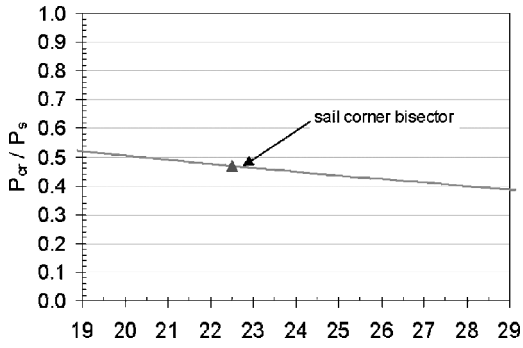

Fig. 12 Ratio of the true buckling load to a simplified buckling load calculation and the effect of halyard angle (deg).

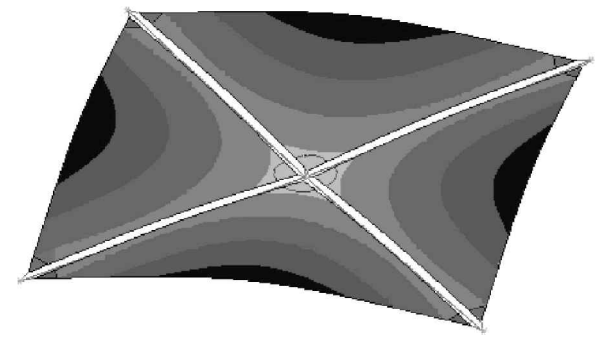

Fig. 13 Lowest system mode.

far the highest load. For example, solar pressure on the sail exerts a tip load 2000 times lower. However, the mast must be analyzed as a beam column (BC), as the deflection from such lateral loads is amplified by the compression imparted by sail tension, to obtain true structural margins.

Similarly for the dynamic analyses of the structure the bending stiffness and natural frequency of the mast are reduced because of the compression imparted by sail tension. This stress-softening effect, which is critical to the correct prediction of the systems lowest mode, is the corollary to the vibration frequency of a string increasing from tensile load. The potential for global curvature is another important consideration in accurate strength margin analysis. The deflection of the boom caused by lateral and compression loading (calculated by the BC method) is amplified by the initial free-state curvature of the mast. Curvature can result from manufacturing tolerances and thermal gradients.

Thermal bending is induced if the sun angle causes one longeron to partially shadow another. The worst-case thermal bending is actually very minor for the gossamer graphite coilable as the longeron CTE is slight and the small diameter of the longeron (relative to the mast diameter) prevents full shadowing. Shadowing can be completely avoided by choosing off-sun orientations that do not match the rare combinations which allow any occulting. In contrast to shell structures, the open trusswork of the coilable is an important structural asset as the prevention of thermal bowing is critical to the margin obtainable in a BC strength analysis of a slender column.

Local curvature of the longeron should be considered in calculations of local buckling load capability, especially for large-scale systems.[6] The present design allows a factor of safety of 7.5 over local buckling (of a longeron within a bay). If mast diameter were increased and longeron diameter decreased, the margins over local and global buckling would converge to result in an optimized mast design. The smaller mast diameter in the present design allowed optimization of the system stowed volume below $\frac{1}{8}$ m^3 and resulted in the larger local buckling margin.

A significant mast loading can arise during the sail deployment if the folds have any tendency to stick together. This loading can be caused by blocking forces, electrostatic charging, or yield stresses induced by packaging with particulate contaminants. An exploratory series of tests was performed to ascertain the pull force of compressed sail folds. Tests were run in vacuum and in air for film to film (back to back) and metal to metal and film to metal over a range of peel angles. Blocking was not evident. The carbon loading was effective in preventing any measurable forces associated with static charge. When scaled to the proposed fold dimensions, the "peel" load for all configurations (with carbon loading) was generally less than 10 mN. It is expected that the addition of slip stitching to provide a deterministic deployment will induce larger loads than fold parting.

Finally, manufacturing tolerances in such a long mast can be a significant concern. In particular, manufacturing tolerances can easily be as large as the BC tip deflection (9 mm) induced by combining all other loadings [e.g., sail tension, solar pressure, and rotational (orientation) acceleration]. Therefore, considering manufacturing tolerances during the design of such a system is important.

S^4 Structure and Sail-Vibration Modes

The tensioned quadrant and stress-softened mast frequencies both are important in the determination of system modes. The vibration modes analysis is further complicated by the need to account for any wrinkled area. The support of the quadrant by three-point tensioning causes compressive second principal stresses in the sail membrane (structural wrinkles). These compressive stresses cause negative eigenvalues and result in chatter modes in a modal analysis. The required methodology is to perform a structural wrinkle region finite element analysis (FEA) analysis first.[3] This analysis corrects the stress distribution to account for wrinkles and eliminates compressive stresses and negative eigenvalues.

The 40-m^2 system's first mode (0.036 Hz) is shown in Fig. 13. The next 10 modes are all below 0.06 Hz. The modes are driven by the sail tension. A minimum biaxial stress at the quadrant center of 10 kPa (1.5 psi) was chosen to ensure that folds would be opened and packaging wrinkles would be stretched sufficiently, as discussed in the next section. Results of prestressed dynamic FEA for the system closely matched simple estimations.

This model is for a free-free system that includes a 140-kg spacecraft on a 2-m offset boom. The cantilever frequency of the tip-weighted boom on the orientation gimbal is >10 times the system frequency, even assuming the same gossamer sail mast design is used for the offset boom. It is the "root" flexibility (the crossed sail masts) that dominates the first mode of the boom.

Sail Flatness and the Effect on Propulsion

An allowance for moderate wrinkles is supported by an analysis of the effect on propulsion. Errors in sail flatness will reduce propulsion as a portion of the momentum transferred by photons reflected at angles others than the mean does not add fully to the desired thrust vector. Wrinkles can be attributed to packaging, structural, and thermal effects.

Material wrinkles are caused by creases induced by the folding and tight compaction of a packaged sail. The "solid fraction" for the current sail construction based on the allocated stowage volume is 18%. This means that folds in the 5-μm (near-term thickness) sail will be separated by 23 μm on average. Although the fold pattern generally prevents stacking of folds and hard creases are not intentionally input during folding, the folds are strained past yield. The sail material has a low modulus and can be easily stretched to a point, which reduces the area affected by the residual strain energy of a hard crease to less than 1% of the distance between folds. The nonflat area on the sail assuming all folds are hard creases is only 4%.

Structural wrinkling arises from the nonuniform stress distribution that exists in the quadrant. The incorporation of catenaries has been baselined in many previous sailcraft designs[7–9] to provide a uniform equal biaxial stress field. It has been assumed that wrinkles would significantly degrade the thrust performance of a sail, and therefore it must be prudent to design to prevent them.[1] However, the methods proposed to avoid structural wrinkles (e.g., catenaries, strip designs, etc.) incur significant weight and manufacturability

penalties. So, completely eliminating wrinkles and maintaining a reasonably light and simple system design are incompatible. In the analysis of the quadrant sail without catenaries, we have been able to demonstrate that although structural wrinkles do arise the effect on thrust is negligible.

The region prone to structural wrinkles lies outside a circle inscribed within the quadrant, as in the photograph of the highly stressed membrane shown in Fig. 14. Analytical tools employed in the past have not provided information as to the number of wrinkles or the amplitude of wrinkles. Lacking this information, it has been assumed that knowledge of the local inclination of a wrinkle (needed to determine how photons reflect) is similarly unknown. But FEA codes used to determine the wrinkled region can in fact reveal useful wrinkle surface inclination information, namely, through the aspect ratio parameter of wrinkle amplitude to wavelength. With this information integration over the wrinkled surface can be performed to find the effective thrust.[3]

The thrust produced by photon reflection pressure can be resolved into two components: a force along the sun line and another tangential to it. The effect of wrinkles on the radial thrust component can be seen in Fig. 15. Interestingly, the radial thrust will increase (neglecting the projected area loss) as the angle of incidence increases. The effect of wrinkles on the tangential thrust is independent of angle of incidence. The reduction grows with wrinkle aspect to 30% at $a/l = 0.2$. For the nominal sail tensioning (10 kPa in the sail center) the predicted wrinkle aspect ratio is less than 0.0005. So, while a reflected image would be distorted if viewed from far away, the effect on thrust is negligible.

The calculations of aspect ratio also allay a previous concern that wrinkles would allow multiple reflections and thus "hot spots" on the sail. For operation at a 40-deg angle of incidence (beyond projected mission needs), it can be shown[3] that the wrinkle aspect would have to be 40 times larger than predicted to result in a light ray reflecting (specularily) to strike the sail a second time.

Work remains to be done in the quantitative assessment of packaging wrinkling. If the packaging volume allotment enforces hard (yielded) creases, these together with the strains from secondary folding (especially in corners) could change the effective constitutive properties of the sail appreciably. Without their inclusion in the modeling, a structural wrinkling analysis might be unconservative. Further development of analytical techniques and/or a dependable dewrinkling agent would be important contributions to further efforts.

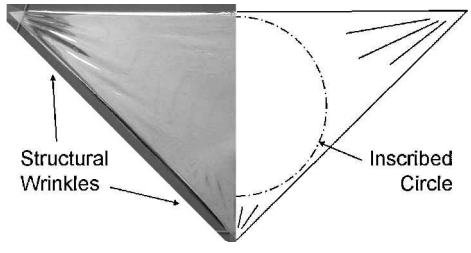

Fig. 14 Structural wrinkles in a highly stressed sail (scale model).

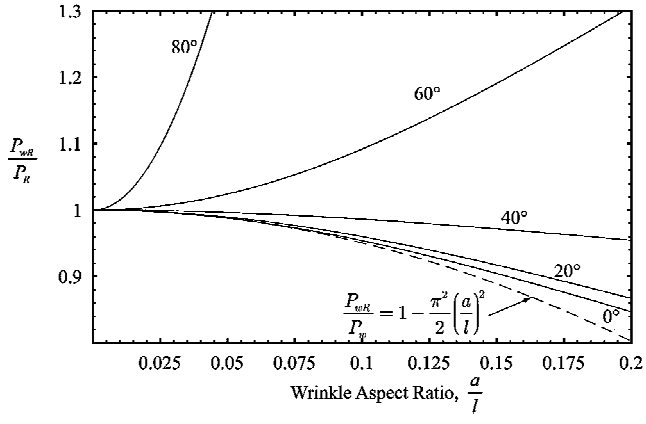

Fig. 15 Effective radial thrust averaged over a wrinkle vs the wrinkle aspect ratio for various angles of incidence.

Table 1 40-m S^4 system mass summary

Component	Mass, kg
Sail assy	12.96
Mast assy	5.76
Stowage structure	3.65
Mechanism, central	1.62
Control mast	1.50
Instrumentation	0.12
Total	24.1

Mass Performance

The mass of the 40-m S^4 system was calculated by summing the known masses of over 70 well-defined parts designed for the application with estimates for the masses of conceptually defined components. The estimated mass breakdown is presented in Table 1. The total estimated mass for the sail system is 24.1 kg, which meets the requirement for the studied mission.

Flight Demonstration and Validation

Objectives

Of key importance to the realization of solar sails is the capability to perform a predictable and controllable deployment of the gossamer sail film and supporting structure in the space environment. This requires development and validation of an ultralightweight, stiff, deployable strut that can be stowed compactly, such as a graphite coilable mast. The thin sail membrane must also be packaged compactly, in a manner that yields controlled deployment, and it must possess sufficient strength margin for the deployment and tensioning loads. Successful completion of a thorough ground-test demonstration and qualification including the primary challenge—deployment—is highly likely given the low risk elements selected for incorporation in the S^4 system and the sequential deterministic plan for deployment.

But solar-sail system technology needs flight validation because of issues introduced by concessions to gravity in deployment offloading. Zero-g deployment behavior and sail shape can never be fully validated by a deployment on Earth. Even with a deterministic deployment, risk exists given that even a small 40-m demonstration sail would be one of the largest space structure ever deployed (five-times greater area than an International Space Station solar-array wing). Flight is required to certify numerous aspects of the system performance such as 1) deployed planarity of the four-mast structure, 2) deployment dynamics of the sails, 3) deployed shape of quadrants, 4) modal behavior of deployed sail and mast structure system, and 5) characteristic acceleration of system.

In addition, the flight dynamics and control of the integrated sail system can only be verified by on-orbit demonstration. Near-Earth perturbations such as magnetic field interaction, gravity gradient torques, and atmospheric drag will be uniquely challenging. Missions will require robust control of the sail thrust vector and the ability to predict and confirm the resultant flight path. Only a free-flying sailcraft can provide the platform to demonstrate those capabilities. A flight validation will provide the demonstration of combined orbital maneuvering and attitude control functions of the solar sail.

A solar-sail technology flight experiment/validation would advance solar sails from concept to a space-proven propulsive subsystem capable of enabling several key missions in NASA's Space Science Enterprise Strategic Plan. Using the sun's constant supply of photons, a solar sail can economically achieve the high delta-V needed to support missions such as the Heliopause Explorer, a precursor mission to Interstellar Probe. Solar sails are uniquely capable of providing the continuous thrust needed to adjust an orbit out of the plane of the ecliptic, thereby enabling Solar Polar Imager, a heliocentric polar orbiter. Other missions in the Living With a

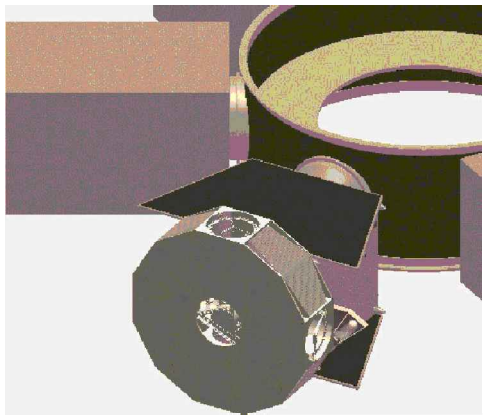

Fig. 16 ST7 in launch slot on ESPA carrier ring.

Star Initiative will require unique vantage points that can only be achieved with a solar sail. Geostorm and similar sentinel-type missions that provide continuous solar monitoring and alerting are only practical with solar sail technology.

Launch Accommodation

NASA has identified several low-cost launch opportunities appropriate for a small system demonstration mission. The baseline proposed to the New Millennium Space Technology 7 (ST7) study program utilized the Evolved Expendable Launch Vehicle (EELV) Secondary Payload Adapter (ESPA). ESPA is a developmental product designed to carry up to six small satellites of up to 180 kg each, along with a 6800-kg primary payload into space on the next generation of U.S. launch vehicles, the EELV. It is designed to provide transportation for secondary payloads as a ride along on the primary payload adaptor ring. As shown in Fig. 16, the standard volume box is exceeded somewhat by the ST7 spacecraft, but the proposed volume is likely within negotiable limits as it does not rise above the primary payload separation plane.

Trajectory Plan

The ESPA flight opportunity, which was targeted for ST7, would have launched the experiment into a super synchronous transfer orbit (SSTO). After separation in SSTO, the perigee would need to be raised to a minimum of 2000 km. A much higher circular (e.g., geostationary) orbit is preferable, as the sail would then not be subjected to gravity gradient and aerodynamic torques. Such influences complicate the control and measurement of solar thrusting. However, the SSTO orbit provides the benefits of a high orbit without the cost of a launch to geosynchronous orbit as $>80\%$ of the time is spent above 30,000 km.

Scalability Demonstration

It is critical that flight validation results be applicable to larger sails with lighter films for the more stressing missions to come. The S^4 design is fully scalable without need for functional reconfiguration. Modeling of performance for sail sizes from 20 to 300 m^2 have been performed. For the data presented next, two key assumptions were made, which emphasize a nominal film stress to straighten out packaging wrinkles and a constant structure margin of safety.

The first is that the quadrant center tensile stress is kept constant at 10 kPa. This causes the halyard tension to increase linearly with sail size. The first mode of the quadrant vs sail size is shown in Fig. 17. The frequency falloff given the constant minimum stress constraint was allowed, as a minimum controllable frequency has not been established. This frequency relation is independent of film thickness (assuming equal stress). Halyard tension would increase proportional to a film thickness change for equal stress.

The second key assumption is that the mast structure factor of safety on buckling is maintained at 3.0. Clearly, as the halyard tension and sail size increase, so must the mast diameter increase to maintain structural margin. The mast diameter vs sail size is shown in Fig. 18, along with the mast slenderness ratio. It is not until the higher sail sizes are challenged that the slenderness ratio will exceed our flight experience. The slenderness ratio of the (three identical) booms on the LACE flight was 192.

Figure 19 shows the generic sailcraft parameter system loading, which is the mass of the sail subsystem and spacecraft divided by the reflective sail area. If combined with the effective reflectivity and the solar flux, the acceleration provided can then be calculated. As bus architecture and payload requirements vary drastically by mission, curves for various spacecraft masses (in kilograms) are given. The performance of the S^4 design alone is fairly constant above 60 m. Larger sail sizes are required to offset increasing spacecraft mass. Increased thrust for a mission is highly dependent on spacecraft mass reduction.

The current performance is already sufficient to meet the most likely first mission, a sentinel position at sub-L_1. As can be seen in Fig. 20, the increase in warning time provided by a 5-μm sail

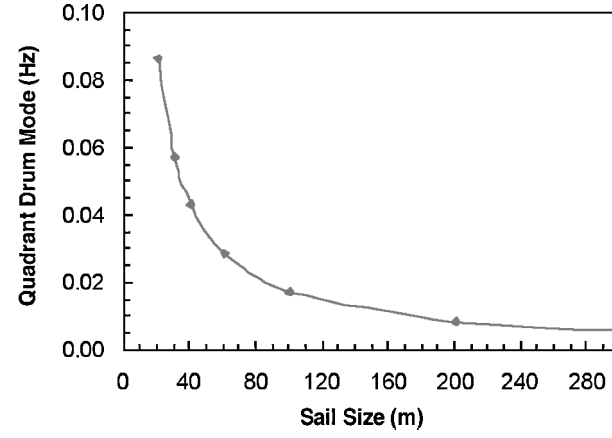

Fig. 17 First mode vs sail size.

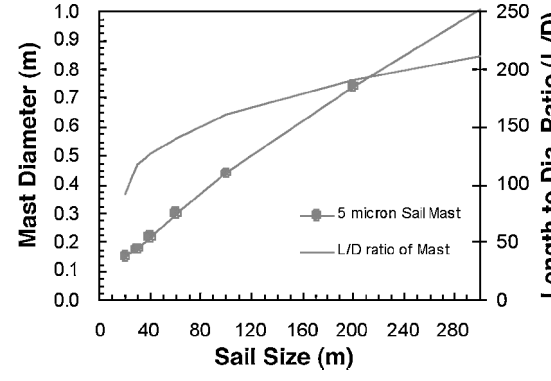

Fig. 18 Mast size vs sail size.

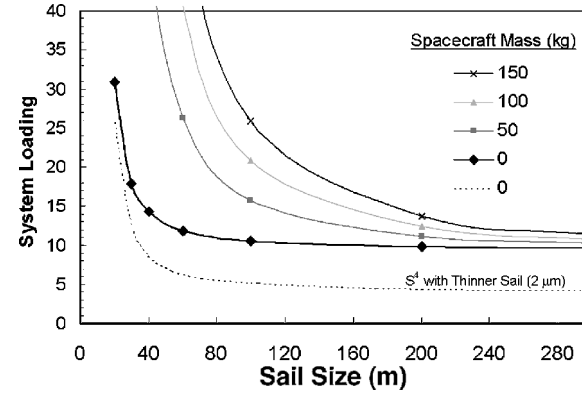

Fig. 19 System loading (g/m^2) vs sail size.

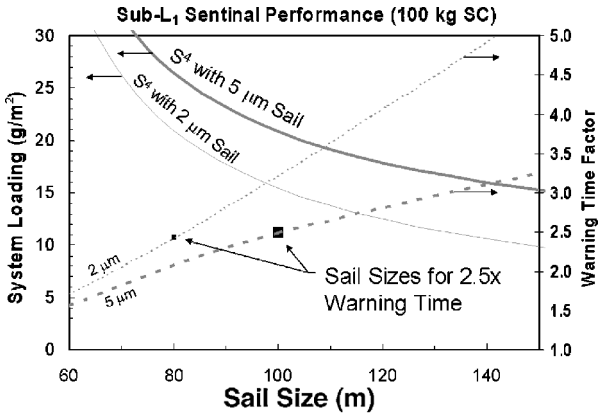

Fig. 20 Sub-L_1 sentinel performance vs sail size and sail thickness.

S^4 propulsion system of 100-m size is 150% (assuming a 100-kg spacecraft). If the thinner sail (targeted at 2 μm) can be demonstrated to be low risk, then the same warning time increase can be achieved with an 80-m sail. The appropriate size of the sail depends on the desired warning time increase and the spacecraft mass. If the mission could be performed with a 50-kg spacecraft (not shown) and only a doubling in warning time was desired, the near-term (5-μm) system size would be only 50 m.

Summary

Solar sails can provide thrust without mass expenditure. The continual acceleration provided by this technology allows cost-effective non-Keplerian paths and unique sentinel perspectives such as a sub-L_1 solar storm observer. A promising system level design for a robust scalable solar propulsion subsystem has been designed and analytically investigated. The technologies selected for the masts, sails, and the system arrangement combine to provide a viable solution to near-term missions. As has been shown, the scalability of the S^4 system allows for more stressing future missions as well. Reduction in sail thickness and advances in payload miniaturization is expected to increase the number of exciting missions best performed with solar sails in the coming years.

The S^4 technology presents a credible low-risk path for component ground development and system validation followed by flight demonstration. The NASA In-Space Propulsion program is leading technology development and demonstration that will soon demonstrate solar-sail subsystems ready for flight validation. NASA has committed to bringing forward this valuable technology as it will surely benefit future U.S. space missions, and it will likely inspire the imagination of the citizenry.

Acknowledgments

The work reported on herein was supported by NASA under a New Millennium Space Technology 7 study program. The support of the Jet Propulsion Laboratory, Pasadena, California, is gratefully acknowledged. Special thanks also to Bob Crawford, Bill Layman, and Martin Mikulas for helpful discussions and technical input.

References

[1]McInnes, C. R., *Solar Sailing: Technology, Dynamics and Mission Applications*, Ist ed., Springer-Verlag, London, 1999, pp. 19–24, 229–270.

[2]Greschik, G., and Mikulas, M. M., "Design Study of a Square Solar Sail Architecture," AIAA Paper 2001-1259, April 2001.

[3]Murphey, T., Murphy, D., Mikulas, M., and Adler, A., "A Method to Quantify the Thrust Degradation Effects of Structural Wrinkles on Solar Sails," AIAA Paper 2002-1560, April 2002.

[4]Mikulus, M., "Structural Efficiency of Long Lightly Loaded Truss and Isogrid Columns for Space Applications," NASA TM-78687, July 1978.

[5]Timoshenko, S. P., and Gere, J. M., *Theory of Elastic Stability*, 2nd ed., McGraw–Hill, New York, 1961, pp. 55–57.

[6]Crawford, R. F., and Hedgepeth, J. M., "Effects of Initial Waviness on the Strength and Design of Built-Up Structures," *AIAA Journal*, Vol. 13, No. 5, 1975, pp. 672–675.

[7]Wright, J. L., *Space Sailing*, 1st ed., Gordon and Breach, Philadelphia, 1992.

[8]Garner, C. E., Layman, W., Gavit, S. A., and Knowles, T., "A Solar Sail Design for a Mission to the Near-Interstellar Medium," Jet Propulsion Lab., Doc. 99-1857, California Inst. of Technology, Pasadena, CA, 1999.

[9]West, J. L., and Derbes, B., "Solar Sail Vehicle System Design for the Geostorm Warning Mission," AIAA Paper 2000-5326, April 2000.

M. S. Lake
Associate Editor